Chemistry–A European Journal
Research Article
doi.org/10.1002/chem.202302544
Chemistry Europe
European Chemical Societies Publishing
www.chemeurj.org

Special Collection

Anion-Dependent Reactivity of Mono- and Dinuclear Boron Cations

Alexander Röther,[a] James C. Farmer,[a] Flavio L. Portwich,[a] Helmar Görls,[a] and Robert Kretschmer*[a, b, c]

Dedicated to Hansjörg Grützmacher, Dietrich Gudat, Evamarie Hey-Hawkins, Manfred Scheer, Rainer Streubel, and Werner Uhl for their contribution to the development of the chemistry of the p-block elements.

The dinuclear bis(*N*-heterocyclic carbene) borane adduct **2** rapidly reacts with tritylium salts at room temperature but the outcome is strongly impacted by the respective counter-ion. Using tritylium tetrakis(perfluoro-*tert*-butoxy)aluminate affords – depending on the solvent – either the bis(boronium) ion **4** or the hydride-bridged dication **5**. In case of tritylium hexafluorophosphate, however, H/F exchange occurs between boron and phosphorus yielding the dinuclear BF_3 adduct **3** along with phosphorus dihydride trifluoride. H/F exchange also takes place when using the mononuclear *N*-heterocyclic carbene BH_3 adduct **6** and hence provides a facile route to PH_2F_3, which is usually synthesized in more complex reaction sequences regularly involving toxic hydrogen fluoride. DFT calculations shed light on the H/F exchange between the borenium ion and the $[PF_6]^-$ counter-ion and the computed mechanism features only small barriers in line with the experimental observations.

Introduction

Carbon-fluorine bond activation by reagents based on main-group elements has drawn increasing attention in the past decade[1] as fluorocarbons are present in a wide range of daily-life products, fine chemicals, and pharmaceuticals.[2] In contrast, the activation of non-carbon-fluorine bonds and fluoride transfer from one main-group element to another is much less explored but has recently gained in importance.[3] The good availability of compounds possessing element-fluorine bonds (E–F with E = main-group element but not carbon) holds significant synthetic value and offers a wide range of applications,[4] including the synthetic use to derive ^{18}F-labelled compounds to be applied in positron-emission tomography (PET).[5] E–F bonds (including E = Al, B, P, Si) are among the strongest known sigma bonds, which is why their activation is often difficult to achieve. However, reports about B–F,[3c,6] P–F,[7] Si–F[1e,8] as well as Sb–F[3c] bond activation are known in the literature. Here, the activation of $[SbF_6]^-$ and $[BF(C_6F_5)_3]^-$, which are usually considered as inert, weakly-coordinating anions, by Lewis acidic stibonium salts deserves particular attention[3c] as it illustrates nicely the capabilities of strong Lewis acids.[9] The capability of a Lewis acid to abstract an F^- from the counter-ion can be judged by its fluoride-ion affinity (FIA), which is also the predominantly applied Lewis-acidity scale.[10] Among the variety of Lewis acidic main-group element compounds, tri-coordinate borenium ions (**A**, Figure 1) have been identified as valuable catalysts and stoichiometric reagents,[11] but their potent electrophilic nature may causes fluoride abstraction from $[BF_4]^-$ and even from tetrakis[3,5-bis(trifluoromethyl)phenyl]-borate.[12] *N*-heterocyclic carbene (NHC) stabilized borenium ions are nowadays well established and their synthesis originates from the respective borane adducts,[13] whereby hydride abstraction gives rise to dinuclear hydride-bridged borenium cations (**B**) and dications (**C**), respectively,[14] which are formed upon dimerization of the mononuclear fragments.

Bis(*N*-heterocyclic carbene)s have been used to frame two (or more) main-group elements within one molecule,[15] but

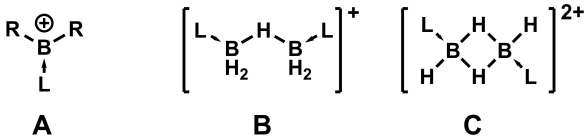

Figure 1. General structure of mononuclear borenium ions (A) and the dinuclear mono- (B) and dications (C); L = Lewis base such as an *N*-heterocyclic carbene.

[a] Dr. A. Röther, J. C. Farmer, F. L. Portwich, Dr. H. Görls, Prof. Dr. R. Kretschmer
Institute of Inorganic and Analytical Chemistry (IAAC)
Friedrich Schiller University Jena
Humboldtstraße 8, 07743 Jena (Germany)
[b] Prof. Dr. R. Kretschmer
Jena Center for Soft Matter (JCSM)
Friedrich Schiller University Jena
Philosophenweg 7, 07743 Jena (Germany)
[c] Prof. Dr. R. Kretschmer
Institute of Chemistry
Chemnitz University of Technology
Straße der Nationen 62, 09111 Chemnitz (Germany)
E-mail: robert.kretschmer@chemie.tu-chemnitz.de

Supporting information for this article is available on the WWW under https://doi.org/10.1002/chem.202302544

Special Collection Part of a Special Collection on the p-block elements.

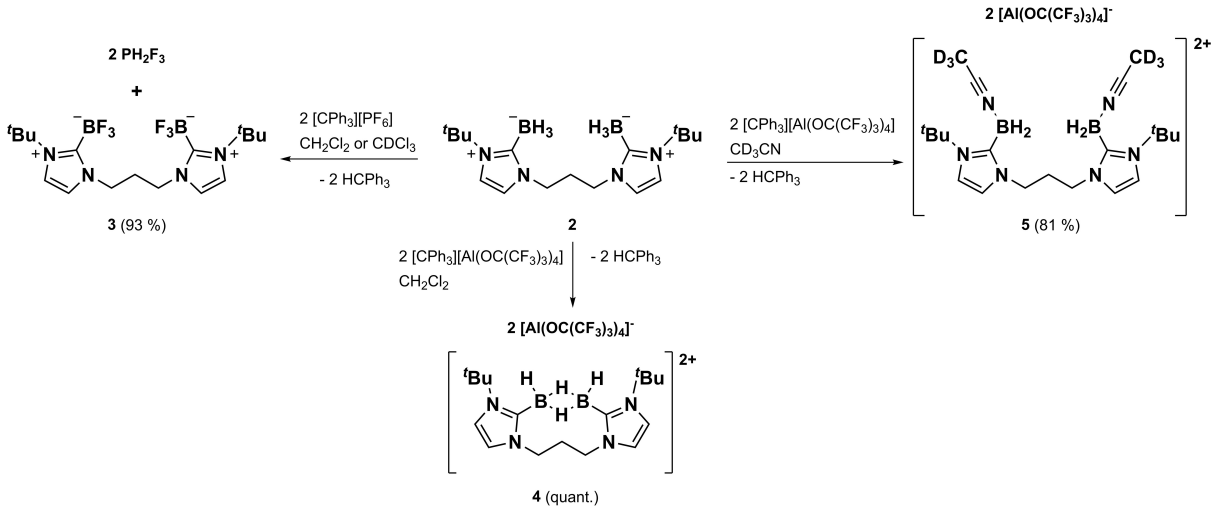

Scheme 1. Reaction of the bis(NHC) borane adduct **2** with tritylium hexafluorophosphate and with tritylium tetrakis(perfluoro-*tert*-butoxy)aluminate.

only a few dinuclear bis(NHC) boranes have been reported in the past.[16] We hence became interested in the synthesis of dinuclear bis(NHC)–BH_3 adducts and subsequent hydride-abstraction reactions as the thus formed borenium centres could possess intramolecular, intermolecular or no hydride-bridges. Our findings on this and the crucial role of the counter-anion are reported herein.

Results and Discussion

The dinuclear propylene-bridged bis(NHC) borane **2** is readily available from the bis(imidazolium salt) **1**, potassium bis(trimethylsilyl) amide (KHMDS), and borane dimethyl sulfide in reasonable yield of 56%. Subsequent reaction of **2** with two equivalents of tritylium hexafluorophosphate, Scheme 1, causes an instantaneous decolourization of the yellow solution. The immediately recorded ^{1}H NMR spectrum shows resonances characteristic for triphenyl methane and an additional distinct set of resonances accounting for the bis(NHC) framework. However, both the ^{11}B and ^{11}B{^{1}H} NMR spectra comprise only one quartet at 0.1 ppm with a coupling constant of 36 *Hz*, which is reminiscent of previously reported mononuclear NHC–BF_3 adducts.[17] The formation of a bis(NHC–BF_3) is further evidenced by a quartet resonating at -133.7 ppm in the ^{19}F NMR spectrum, a value in the range typically reported for NHC–BF_3 adducts,[6,17] and finally, by means of single-crystal X-ray diffraction analysis; the molecular structures of **2** and **3** in the solid state are given in Figure 2.

Notably, B–H free products were previously observed when Lewis-base BH_2R adducts (R=H, aryl) were reacted with tritylium tetrafluoroborate.[18] In case of NHC–BH_2Ar, Lacôte and co-workers proposed an initial borenium ion formation, which then abstracts a fluoride from $[BF_4]^-$ forming NHC–BHFAr and BF_3.[18b] In case of electron-rich arenes, BHFAr is replaced by the more Lewis-basic BF_3, while with electron-poor arenes, free BF_3 has been trapped with phenol and the thereby formed hydrogen fluoride gives rise to a subsequent acid-base reaction forming NHC–BF_2Ar. As the hexafluorophosphate anion is the only conceivable fluorine source in here and as conceivable phosphorus containing products may be volatile, the reaction was repeated as in situ experiments in J. Young NMR tubes. Inspection of the ^{31}P spectrum reveals the absence of $[PF_6]^-$, but both the ^{31}P and ^{31}P{^{1}H} spectra were rather complex showing multiple signals ranging from −238 to 197 ppm. Based on the ^{31}P NMR spectra we assumed the formation of PH_xF_{5-x} derivatives, which are known to readily react with glass forming a variety of products.[19] Hence, we repeated the experiments in a glovebox using a polypropylene vial and the solution was immediately transferred to a thin-walled PTFE tube. Now, a quartet of triplets at −26.0 ppm ($^{1}J_{P\text{-}F}$ = 877 Hz, $^{1}J_{P\text{-}H}$ = 850 Hz) was observed in the ^{31}P NMR spectrum, which collapsed to a

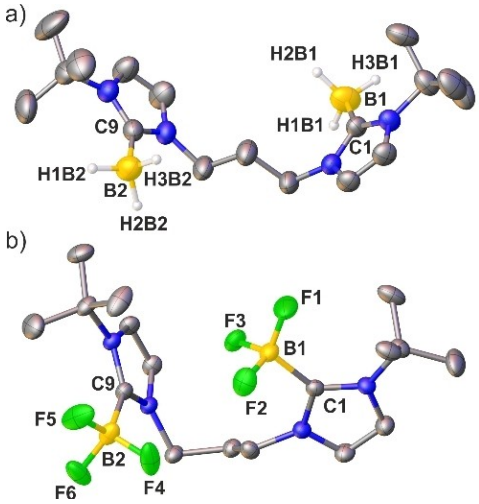

Figure 2. Solid-state structures (hydrogen atoms except the BH and a second, disordered part of F4-F6 are omitted for the sake of clarity) with selected bond lengths [Å] and angles [°] of a) **2**: B1–C1 1.606(4), B1–H1B1 1.07(4), B1–H2B1 1.13(4), B1–H3B1 1.09(4), B2–C9 1.601(5), C1–B1–H1B1 106(2), H1B1–B1–H2B1 112(3); b) **3**: B1–C1: 1.671(3), B1–F1: 1.376(3), N2–C1–N1: 105.66(15), F1–B1–C1: 114.95(17), F1–B1–F2: 109.17(19).

quartet upon proton-decoupling, Figures S32–S34, indicating the presence of two P–H bonds. The in situ ^{1}H NMR spectrum, Figure S31, shows only three sets of signals, i.e., those accounting for **3** and triphenylmethane, respectively, and a doublet of quartet as expected for PH_2F_3. These data are in good agreement with previously reported spectra[19b,20] and dynamic NMR calculations[21] of PH_2F_3, and evidence that H/F-exchange between the boron atoms of **2** and the phosphorus centre of $[PF_6]^-$ gives rise to **3** and PH_2F_3 besides the formation of triphenylmethane. As **3** was isolated in 93% yield, we also attempted to quantify the formation of PH_2F_3, which is challenging because of its low boiling point of 277 K and its reactivity towards glassware. Hence, the in situ ^{1}H NMR experiments have been repeated at 233 K using the procedure described above (PTFE tube and sample preparation in a polypropylene vial but using CD_2Cl_2 as solvent) and triphenylene has been added as an internal standard. Based on the integrals of the undisturbed ^{1}H NMR resonances, yields between 65 and 83% after 1 h could be recognized, Figures S36–37.

When performing the in situ experiments in acetonitrile-d_3, the respective ^{1}H, ^{11}B, ^{13}C, ^{19}F, and ^{31}P NMR spectra obtained immediately after sample preparation, Figures S38-S42, show no evidence for the formation of either **3** or PH_2F_3. While the starting material **2** is not fully consumed, formation of triphenylmethane is evidenced by the typical resonances in the ^{1}H NMR spectrum and the ^{11}B NMR data hint towards the formation of a boronium complex likely to be formed upon reaction of an intermediary borenium ion with CD_3CN (see below). The $[PF_6]^-$ counter-ion appears to be intact according to its ^{31}P NMR signal. However, after 18 h, full consumption of **2** but also the formation of **3** can be recognized from the ^{1}H and ^{11}B NMR spectra, Figure S43–44.

As the $[PF_6]^-$ counter-ion appeared to be not suitable for dinuclear boron cations, we next investigated the reactivity of **2** towards tritylium tetrakis(perfluoro-*tert*-butoxy)-aluminate,[22] Scheme 1. Independent of the solvents used, i.e., $CDCl_3$ or CD_3CN, the ^{1}H, ^{11}B, and ^{19}F NMR spectra show no signals accounting for the formation of **3**. Instead, the observed solvent-dependent ^{11}B resonances, i.e., −16.5 ppm in $CDCl_3$ and −22.7 ppm in acetonitrile-d_3, are reminiscent of borenium and boronium ions, respectively.[14] After a short work-up, the dinuclear dications **4** and **5** could be isolated in 81% and quantitative yield, respectively, and the obtained single-crystals allowed us establishing their molecular structures in the solid state, Figure 3. Please note that a relatively high R-factor is associated with these structures due to extensive disorder in the tetrakis(perfluoro-*tert*-butoxy)-aluminate counter-ion. **4** features a central B(μ-H)$_2$B core and the tetrahedral coordination environment of boron is completed by a terminal hydride and a NHC unit each. In contrast to the previously reported bis(borenium) ion formed upon dimerization,[14b] the two terminal hydrides and the two NHC fragments are *cis*-oriented with respect to each other. However, the intramolecular formation of the B(μ-H)$_2$B unit cannot compete with stabilization gained by coordination to acetonitrile-d_3, as evidenced by the molecular structure of **5**. Hence, **5** possesses two non-bridged boronium ions which are four-fold coordinated by two hydride ligands, one molecule of acetonitrile, and one NHC unit, reminiscent of a previously reported boronium ion stabilized by ammonia and an NHC.[23]

These experimental findings provide valuable insight into the reactivity of bis(NHC)-stabilized bis(borenium) ions: *i*) bis(borenium) ions formed by hydride abstraction have a stronger fluoride-ion affinity (FIA) than PF_5. *ii*) An NHC–PF_5 adduct is not obtained although, based on computational[24,10] and experimental[25] fluoride-ion affinity (FIA) scales, PF_5 is the stronger Lewis acid than BH_3 or BF_3 (and consequently the intermediates BH_xF_{3-x}), which indicates kinetic stabilization. *iii*) Donor solvents such as acetonitrile initially trap the formed bis(borenium) as bis(boronium) ions, but subsequent reactions with the $[PF_6]^-$ counter-ion take place. *iv*) C–F bond activation of tetrakis(perfluoro-*tert*-butoxy)-aluminate by bis(borenium) ions is not observed under the experimental conditions.

In order to check if the H/F exchange is limited to dinuclear boranes based on bis(NHC)s, we also conducted in situ experiments of tritylium hexafluorophosphate with 1,3-bis(*tert*-butyl)imidazol-2-ylidene borane **6** and commercial borane dimethyl sulfide complex **7**, respectively, in $CDCl_3$, Scheme 2. In both cases, we could identify the BF_3-containing products **8** and **9**, respectively, based on their ^{1}H, ^{11}B, and ^{19}F NMR spectra.[26] However, the ^{31}P NMR spectra differ to quite some extent: when using the NHC borane **6**, PH_2F_3 was identified as the major and almost exclusive product, Figure S47, while the reaction with borane dimethyl sulfide complex gives rise to a complex mixture with only small amounts of PH_2F_3, Figure S51. In consequence and although not commercially available, **6** is the better source to generate PH_2F_3 using the protocol reported in here.

Aiming to rationalize the experimental findings, the reaction of **6** with tritylium hexafluorophosphate was modelled by

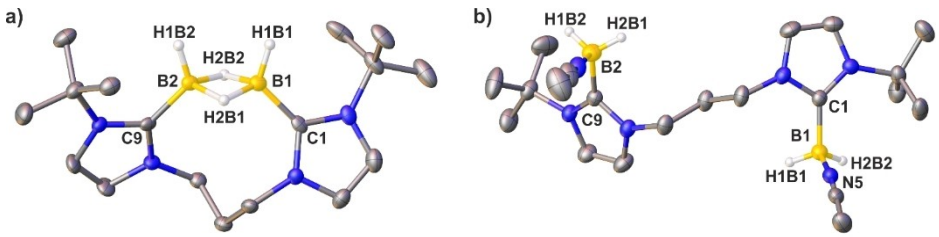

Figure 3. Solid-state structures of a) **4** and b) **5** (counter-ions and hydrogen atoms except the BH are omitted for the sake of clarity). Selected bond lengths [Å] and angles [°] of: (a) **4**: B1–C1 1.566(6), B2–C9 1.573(5), B1–H1B1 1.06(4), B1–H2B1 1.30(3), H1B1–B1–H2B1 111(3); (b) **5**: B1–C1 1.608(4), B2–C9 1.612(4), B1–H1B1 0.990(3), B1–H2B1 0.990(3), B1–N5 1.573(4), H1B1–B1–H2B1 108.2(3), C1–B1–N5 109.5(2).

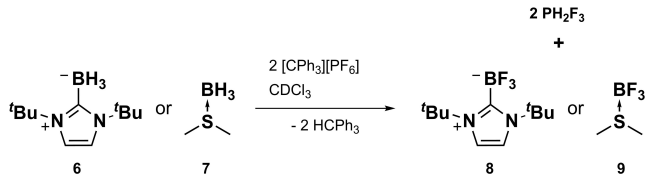

Scheme 2. Reactions of Lewis-base stabilized boranes **6** and **7** with tritylium hexafluorophosphate.

means of density functional theory (DFT) calculations at the BP86(GD3-BJ)/aug-cc-pVTZ level of theory.[27] Notably, hydride transfer from amine boranes to carbenium ions has been studied experimentally before and was found to proceed through a polar mechanism, in which the migrating hydride is partly bound to both the boron and the carbon atom in the postulated transition structure.[28]

Mechanistically, the reaction consists of a series of three fluoride-ion transfer steps, which are subsequently discussed next, Figure 4 and S54 as well as Table S2. After the initial formation of a borenium ion, association of PF_6 yields the encounter complex **Int1**, in which one of the P–F bonds is activated upon coordination to the borenium centre as illustrated by elongation of the respective P–F bond (1.93 Å). P–F bond cleavage occurs via the transition structure **TS1** and the resulting PF_5 fragment is simultaneously transferred onto a neighbouring boron bound hydride. Please note that this step, associated with a free energy of activation of 45.8 kJ mol^{-1}, is the energetically most demanding on the potential-energy surface towards the product complex **Prod** and in consequence, rate limiting. In the thus formed intermediate (**Int2**), the B–H···PF_5 unit resides in the plane of the NHC and steric repulsion of the neighbouring *tert*-butyl groups prevent an extensive P–H interaction as shown by an elongated bond distance of 1.70 Å. In order to facilitate the dissociation of the PHF_5 fragment, the boron unit is rotated about the C–B bond (**TS2**, 8.0 kJ mol^{-1}) to a more favourable position between the *tert*-butyl groups (**Int3**), resulting in a shorter P–H bond of 1.58 A. Finally, PHF_5 is released from the borenium centre via **TS3** (16.9 kJ mol^{-1}) yielding the weakly associated intermediate complex **Int4**, which formation is overall exergonic by 35.2 kJ mol^{-1} relative to **Int1**.

The thus formed PHF_5 has two different kinds of fluorine atoms, i.e., *cis* or *trans* oriented with respect to the proton, and two mechanistic scenarios for the second H/F exchange might be operative: Both pathways are associated with small barriers that are lower in free energy than the preceding **TS1**, which is why a differentiation is not possible. Furthermore, as both scenarios are mechanistically comparable, only the *cis* pathway, Figure 4, is discussed next while the discussion of the *trans* path is described in the Supporting Information. Abstraction of a *cis* fluoride originates from the related encounter complex **Int5$_{cis}$** (−78.8 kJ mol^{-1} relative to **Int1**) in which a *cis* fluoride is directed towards the borenium centre. From here, B–F bond making and P–F bond breaking take place via **TS5$_{cis}$**, associated with only a small barrier of 11.5 kJ mol^{-1} affording **Int6$_{cis}$** in which the PHF_4 unit is weakly associated with the thus formed NHC-stabilized BHF_2 centre. Rotation of the PHF_4 moiety in such a way that the P-bound hydrogen atom can form a hydrogen bond with the abstracted F is associated with a marginable barrier of 4.2 kJ mol^{-1} (**TS6$_{cis}$**) yielding **Int7$_{cis}$**. Further rotation of the PHF_4 fragment via **TS7$_{cis}$** causes a pre-orientation of the remaining B-bound hydride onto the axial position of PHF_4 whilst keeping the PH···F hydrogen bond intact and forming **Int8$_{cis}$**. In order to cleave off PH_2F_4, rotation of the BF_2-H···PHF_4 unit (**TS8$_{cis}$**) is necessary affording **Int9$_{cis}$**, from which B–H bond breaking and P–H bond making finally proceeds via **TS9$_{cis}$** by formation of the associate complex **Int10$_{cis}$**. From here, a final P–F bond activation step (**TS10$_{cis}$**) associated with fluoride transfer from phosphorus to the borenium centre gives the product complex **Prod** consisting of **8** and PH_2F_3, in which both hydrogen atoms reside in equatorial position. The overall

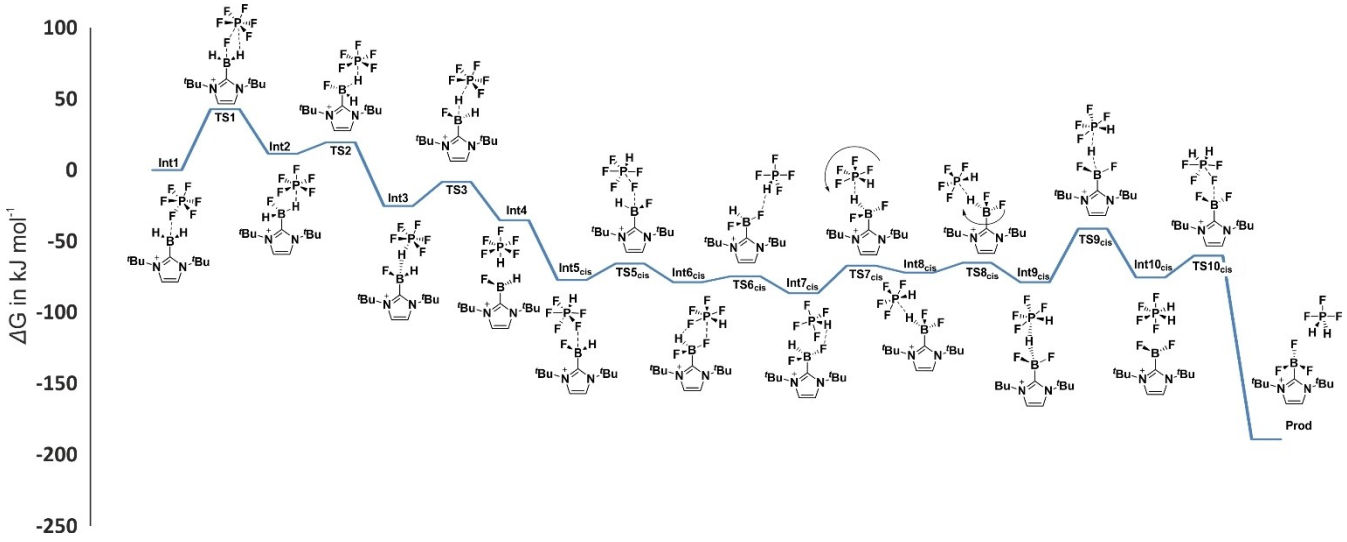

Figure 4. Schematic potential-energy surface with Gibbs free energies (given in kJ mol^{-1}) calculated at the BP86(GD3BJ)/aug-cc-pVTZ level of theory for the formation of **8**; the energy values are given in Table S2 and the pathway of the abstraction of the *trans* hydrogen of PHF_4 is shown in Figure S56.

process in going from **Int1** to **Prod$_s$** is exergonic by −189.2 kJ mol^{-1}.

Conclusions

In summary, the unprecedented dinuclear bis(boronium) ion **4** and the dicationic hydride-bridged compound **5** are synthetically accessible by reacting tritylium tetrakis(perfluoro-*tert*-butoxy)-aluminate with the bis(NHC)–BH_3 adduct **2** in dichloromethane and acetonitrile, respectively. In contrast, performing the reaction with tritylium hexafluorophosphate gives rise to PH_2F_3 and the dinuclear boron trifluoride complex **3**. Clean H/F exchange is also observed when reacting the readily available mononuclear NHC–BH_3 adduct **6** with tritylium hexafluorophosphate while the reaction with the commercially available borane dimethyl sulfide complex **7** gives complex reaction mixtures. Hence, the protocol involving **6** and $[CPh_3][PF_6]$ offers a convenient synthetic route towards PH_2F_3 and does not require aggressive or toxic reagents. In view of the previously reported syntheses of PH_2F_3 that include the reaction of HF with either H_3PO_2 or H_3PO_2,[19a,29] reactions of $(CH_3)_3SnH$ with PF_5[19b] or reactions of NaH_2PO_2 with HSO_3F,[30] phosphorus dihydride trifluoride is accessible in a safer and greener fashion. Furthermore, as the fluoride transfer is fast, it might be suitable to access ^{18}F-labelled Lewis-base stabilized BF_3 adducts starting from ^{18}F-hexafluorophosphate,[31] and may be hence suitable for application in PET imaging,[32] where the moderate half-life of ^{18}F (109.8 min) necessitates facile procedures. The underlying reaction mechanism have been investigated by means of DFT calculations and the conceivable pathways for the H/F exchange between the borenium ion and $[PF_6]^-$ are associated only with small barrier according to the calculations.

Experimental and Computational Section

General experimental procedure

All preparations were performed under an inert atmosphere of dinitrogen by means of Standard Schlenk-line or glovebox (GS-Systemtechnik and MBraun) techniques. Ethylene glycol dimethyl ether, toluene and *n*-hexane were used as p.a. grade and distilled from Na/benzophenone prior to use. Acetonitrile and dichloromethane were used as p.a. grade and distilled from calcium hydride and phosphorus pentoxide, respectively. Acetonitrile-d_3, bromobenzene, and $CDCl_3$ were dried over molecular sieves (3 Å) prior to use. Borane dimethyl sulfide and triphenylcarbenium hexafluorophosphate were obtained from Sigma Aldrich while triphenylcarbenium tetrakis(perfluoro-*tert*-butoxy)aluminate was received from Ionic Liquid Technologies (IoLiTec) GmbH. *tert*-butyl imidazole and 1,3-bis(*tert*-butyl)imidazol-2-ylidene borane were synthesized according to literature procedures.[33]

Synthesis

1: The synthesis was performed according to a modified literature procedure,[34] i.e., *tert*-butyl imidazole (18.26 g, 147 mmol) and 1,3-dibromopropane (7.5 mL, 74 mmol) were dissolved in THF (50 mL) and heated to reflux. A colourless solid precipitated from the solution and the reaction was stopped after 20 h. The solids were filtered off and dried in vacuum yielding a colourless solid; 32.98 g, 74 mmol, 99%. The ^{1}H and ^{13}C{^{1}H} NMR spectra were in accordance with the literature:[3] ^{1}H NMR (400 MHz, $CDCl_3$) δ = 1.70 (s, 18 H), 2.99 (quin, *J* = 7.53 Hz, 2 H), 4.73 (t, *J* = 7.60 Hz, 4 H), 7.37 (t, *J* = 1.90 Hz, 2 H), 8.17 (t, *J* = 1.75 Hz, 2 H), 10.31 (t, *J* = 1.61 Hz, 2 H). ^{13}C{^{1}H}-APT NMR (151 MHz, $CDCl_3$) δ = 30.0 (+, CH_3, *t*Bu), 31.0 (quaternary, *t*Bu), 46.9 (−, CH_2), 60.4 (−, CH_2), 118.9 (+, CH), 123.9 (+, CH), 135.2 (−, NC(H)N). ATR-IR [cm^{-1}] = 3388.15, 3337.83, 3263.28, 3134.69, 3063.87, 2970.69, 1647.48, 2877.50, 1559.89, 1552.44, 1457.39, 1375.39, 1241.20, 1205.79, 1136.84, 1121.93, 827.47, 812.56, 767.83, 751.06, 656.01. ESI(+)HRMS: calcd. $C_{17}H_{30}N_4^{2+}$ $[M]^{2+}$ 145.1230, found 145.1231.

2: Bis(imidazolium salt) **1** (4.13 g, 9.2 mmol) and sodium bis(trimethylsilyl)amide (3.70 g, 20.24 mmol) were added to a Schlenk flask and cooled to −50 °C. Ethylene glycol dimethyl ether (40 mL) was added and the resulting suspension was warmed to room temperature and stirred for two hours. Then, the solvent was evaporated and the residue was treated with toluene (15 mL) and hexane (50 mL). The resulting suspension was stirred for 5 min, then, the solids were allowed to settle down and the supernatant was filtrated. This extraction procedure was repeated for one time. Borane dimethyl sulfide (1.75 mL, 18.4 mmol) was added to the filtrate causing incipient precipitation of a colourless solid. This suspension was stirred for one hour at room temperature before the solids were filtered off and recrystallized from ethanol. **2** was obtained as colourless, needle-shaped crystals suitable for x-ray analysis. 1.62 g, 5.12 mmol, 56%. ^{1}H NMR (400 MHz, $CDCl_3$) δ = 0.81–1.62 (m, 6H), 1.73 (s, 18H), 2.29–2.42 (m, 2H), 4.14–4.30 (m, 4H), 6.88 (d, *J* = 2.05 Hz, 2H), 6.98 (d, *J* = 2.05 Hz, 2H). ^{1}H{^{11}B} NMR (400 MHz, $CDCl_3$) δ = 1.01–1.49 (m, 6H), 1.73 (s, 18H), 2.35 (quin, *J* = 7.41 Hz, 2H), 4.22 (t, *J* = 7.34 Hz, 4H), 6.88 (d, *J* = 2.05 Hz, 2H), 6.98 (d, *J* = 2.05 Hz, 2H). ^{11}B NMR (128 MHz, $CDCl_3$) δ = −34.20 (q, *J* = 86.86 Hz). ^{11}B{^{1}H} NMR (128 MHz, $CDCl_3$) δ = −34.19 (s).^{13}C{^{1}H}-APT NMR (101 MHz, $CDCl_3$) δ = 29.6 (−, CH_2) 29.7 (+, CH_3, *t*Bu) 46,0 (−, CH_2) 59.2 (quaternary, *t*Bu), 116.6 (+, CH) 118.1 (+, CH). ATR-IR [cm^{-1}] = 3171.96, 3140.28, 2978.14, 2966.96, 2918.51, 2879.37, 2359.40, 2279.27, 2227.08, 1483.48, 1466.71, 1425.71, 1397.75, 1388.43, 1366.07, 1339.98, 1271.02, 1228.16, 1215.11, 1192.75, 1164.79, 1123.79, 1095.84, 1071.61, 1054.84, 1032.47, 929.97, 874.06, 749.20, 706.33, 656.01. ESI(+)HRMS: calcd. for $C_{17}H_{33}B_2N_4$ $[M-H^-]^+$ 315.2886, found 315.2891.

3: **2** (173.0 mg, 0.55 mmol) was dissolved in 5 mL of dichloromethane and added to a Schlenk flask containing triphenylcarbenium hexafluorophosphate (425.0 mg, 1.09 mmol). Gas evolution was observed and the yellow reaction mixture turned colourless within one minute. ^{1}H, ^{11}B, and ^{13}C NMR analysis confirmed full conversion of **2** to the product **3**. Colourless needle-shaped crystals suitable for x-ray analysis were grown from the DCM solution by layering with *n*-hexane; 216 mg, 0.51 mmol, 93%. ^{1}H NMR (400 MHz, $CDCl_3$) δ = 1.73 (s, 18H) 2.48 (quin, *J* = 7.45 Hz, 2H) 4.13–4.61 (m, 4H) 7.06 (d, *J* = 2.05 Hz, 2H) 7.15 (d, *J* = 2.05 Hz, 2H). ^{1}H {^{11}B} NMR δ = 1.73 (s, 18 H) 2.48 (quin, *J* = 7.41 Hz, 2H) 4.39 (t, *J* = 7.48 Hz, 4H) 7.06 (d, *J* = 1.76 Hz, 2H) 7.15 (d, *J* = 1.76 Hz, 2H). ^{11}B NMR (128 MHz, $CDCl_3$) δ = −0.13 (q, *J* = 35.60 Hz). ^{11}B{^{1}H} NMR (128 MHz, $CDCl_3$) δ = −0.13 (q, *J* = 36.00 Hz). ^{13}C-APT NMR (101 MHz, $CDCl_3$) = 30.5 (+, CH_3, *t*Bu) 31.9 (quaternary, *t*Bu), 47.6 (−, CH_2) 60.89 (−, CH_2) 118.48 (+, CH) 120.15 (+, CH). ^{19}F NMR (376 MHz, $CDCl_3$) δ = −133.73 (br dd, *J* = 70.64, 33.91 Hz). ATR-IR [cm^{-1}] = 3190.6, 3151.5, 3125.4, 2970.7, 2940.9, 1477.9, 1425.7, 1237.5, 1222.6, 1207.7, 1198.3, 1155.5, 1062.3, 1030.6, 918.8, 883.38, 725.0. ESI(+)HRMS: calcd. For $C_{17}H_{29}BF_3N_4^+$ $[M-BF_3+H^+]^+$ 357.2432, found 357.2436, calcd. for $C_{17}H_{28}B_2F_6N_4Na^+$ $[M+Na^+]^+$ 447.2296 found 447.2306. Elemental analysis, calcd. for $C_{17}H_{28}B_2F_6N_4$, C 48.15, H 6.66, N 13.21, found C 47.95, H 6.71, N 12.88.

4: **2** (38.3 mg, 0.12 mmol) was dissolved in 5 mL of dichloromethane and a solution of triphenylcarbenium tetrakis(perfluoro-*tert*-butoxy)aluminate (293.0 mg, 0.82 mmol) in 5 mL of dichloromethane was added. The yellow colour of the reaction mixture disappeared within seconds. The solvent was removed *en vacuo*, the remaining colourless solid was washed three times with *n*-hexane (3 mL each) and dried in vacuum; 269 mg, 0.12 mmol, quantative. Crystals suitable for X-ray analysis were obtained from a concentrated bromobenzene solution upon storage at −39 °C.^{1}H NMR (400 MHz, $CDCl_3$) $\delta = 1.77$ (s, 18H), 2.38 (dt, $J = 10.89$, 5.52 Hz, 2 H), 2.44–3.38 (m, 3H), 4.07 (br s, 4 H), 7.07 (d, $J = 2.05$ Hz, 2 H), 7.37 (d, $J = 2.05$ Hz, 2H).^{1}H{^{11}B} NMR (400 MHz, $CDCl_3$) $\delta = 1.77$ (s, 18H), 2.38 (dt, $J = 10.49$, 5.47 Hz, 2H), 2.69 (br s, 4H), 4.08 (br s, 4H), 7.07 (d, $J = 1.76$ Hz, 2H), 7.38 (d, $J = 1.76$ Hz, 2 H).^{11}B NMR (128 MHz, $CDCl_3$) $\delta = 16.5$ (br s). ^{11}B{^{1}H} NMR (128 MHz, $CDCl_3$) $\delta = 16.5$ (s). ^{13}C-APT NMR $\delta = 30.1$ (+, CH_3, *t*Bu) 32.4 (quaternary, *t*Bu), 43.2 (−, CH_2) 61.3 (−, CH_2) 119.0 (+, CH) 120.6 (+, CH), 121.2 (−, q, $J = 294.0$ MHz, CF_3). ATR-FTIR [cm^{-1}] = 2991.19, 2948.32, 2512.23, 2465.63, 2361.27, 2338.90, 1351.16, 1297.11, 1272.89, 1230.02, 1207.66, 1166.66, 1107.02, 967.24, 831.20, 724.97.

5: **2** (14.8 mg, 0.047 mmol) was dissolved in 3 mL of deuterated acetonitrile and a solution of triphenylcarbenium tetrakis(perfluoro-*tert*-butoxy) aluminate (113.3 mg, 0.94 mmol) in 3 mL of deuterated acetonitrile was added. Gas evolution was observed and the yellow reaction mixture turned colourless within seconds. The solvent was removed *en vacuo*, the remaining colourless solid was washed three times with *n*-hexane (3 mL each) and dried in vacuum; 89.2 mg, 0.038 mmol, 81 %. Colourless needle-shaped crystals suitable for an X-ray analysis were grown from the NMR sample upon layering the CD_3CN solution with *n*-hexane and storage at −40 °C. ^{1}H NMR (400 MHz, CD_3CN) $\delta = 1.70$ (s, 18H) 2.24–2.37 (m, 2H) 4.15–4.30 (m, 4H) 7.30 (d, J = 2.05 Hz, 2H) 7.45 (d, J = 2.05 Hz, 2H). ^{1}H{^{11}B} NMR (400 MHz, CD_3CN) $\delta = 1.70$ (s, 18H), 2.32 (quin, $J = 7.56$ Hz, 2H), 2.66 (br s, 4H), 4.24 (t, $J = 7.48$ Hz, 4H), 7.30 (d, $J = 2.05$ Hz, 2H), 7.45 (d, $J = 2.05$ Hz, 2H). ^{11}B NMR (128 MHz, CD_3CN) $\delta = -22.68$ (br s). ATR-FTIR [cm^{-1}] = 2985.60, 2950.19, 2361.27, 2337.04, 1351.16, 1297.11, 1272.89, 1239.34, 1207.66, 1166.66, 1107.02, 967.24, 831.20, 754.79, 724.97, 698.88.

Deposition Numbers 2090256 (for **2**), 2090257 (for **3**), 2090258 (for **4**), 2090259 (for **5**) contain the supplementary crystallographic data for this paper. These data are provided free of charge by the joint Cambridge Crystallographic Data Centre and Fachinformationszentrum Karlsruhe Access Structures service.

Supporting Information

The authors have cited additional references within the Supporting Information.[35]

Acknowledgements

The project was financially supported by the Deutsche Forschungsgemeinschaft (DFG, KR4782/3-1) and the Friedrich Schiller University Jena. We thank the Rechenzentrum of the Friedrich Schiller University Jena for the allocation of computer time and Dr. Daniel Kratzert for assistance with the crystallographic analysis. Open Access funding enabled and organized by Projekt DEAL.

Conflict of Interests

The authors declare no conflict of interest.

Data Availability Statement

The data that support the findings of this study are available in the supplementary material of this article.

Keywords: bond activation · boron · cation · Lewis base · phosphorus

[1] a) T. Stahl, H. F. T. Klare, M. Oestreich, *ACS Catal.* **2013**, *3*, 1578–1587; b) G. Coates, F. Rekhroukh, M. R. Crimmin, *Synlett* **2019**, *30*, 2233–2246; c) O. Kysliak, H. Görls, R. Kretschmer, *Chem. Commun.* **2020**, *56*, 7865–7868; d) M. Talavera, G. Meißner, S. G. Rachor, T. Braun, *Chem. Commun.* **2020**, *56*, 4452–4455; e) E. Pietrasiak, E. Lee, *Synlett* **2020**, *31*, 1349–1360; f) O. Kysliak, H. Görls, R. Kretschmer, *J. Am. Chem. Soc.* **2021**, *143*, 142–148.

[2] a) H. Amii, K. Uneyama, *Chem. Rev.* **2009**, *109*, 2119–2183; b) T. Ahrens, J. Kohlmann, M. Ahrens, T. Braun, *Chem. Rev.* **2015**, *115*, 931–972.

[3] a) J. Bauer, H. Braunschweig, K. Kraft, K. Radacki, *Angew. Chem. Int. Ed.* **2011**, *50*, 10457–10460; b) J. Bauer, H. Braunschweig, R. D. Dewhurst, K. Radacki, *Chem. Eur. J.* **2013**, *19*, 8797–8805; c) B. Pan, F. P. Gabbaï, *J. Am. Chem. Soc.* **2014**, *136*, 9564–9567; d) F. Buß, C. Mück-Lichtenfeld, P. Mehlmann, F. Dielmann, *Angew. Chem. Int. Ed.* **2018**, *57*, 4951–4955; e) P. Tomar, T. Braun, E. Kemnitz, *Chem. Commun.* **2018**, *54*, 9753–9756; f) D. J. Sheldon, M. R. Crimmin, *Chem. Commun.* **2021**.

[4] a) G. E. Smith, H. L. Sladen, S. C. G. Biagini, P. J. Blower, *Dalton Trans.* **2011**, *40*, 6196–6205; b) V. Bernard-Gauthier, C. Wängler, E. Schirrmacher, A. Kostikov, K. Jurkschat, B. Wängler, R. Schirrmacher, *BioMed Res. Int.* **2014**, *2014*, 454503.

[5] a) S. M. Ametamey, M. Honer, P. A. Schubiger, *Chem. Rev.* **2008**, *108*, 1501–1516; b) M. M. Alauddin, *Am. J. Nucl. Med. Mol. Imaging* **2012**, *2*, 55–76; c) D. M. Perrin, *Acc. Chem. Res.* **2016**, *49*, 1333–1343; d) M. G. Campbell, J. Mercier, C. Genicot, V. Gouverneur, J. M. Hooker, T. Ritter, *Nat. Chem.* **2016**, *9*, 1–3; e) D. van der Born, A. Pees, A. J. Poot, R. V. A. Orru, A. D. Windhorst, D. J. Vugts, *Chem. Soc. Rev.* **2017**, *46*, 4709–4773; f) X. Deng, J. Rong, L. Wang, N. Vasdev, L. Zhang, L. Josephson, S. H. Liang, *Angew. Chem. Int. Ed.* **2019**, *58*, 2580–2605.

[6] D. J. Nielsen, K. J. Cavell, B. W. Skelton, A. H. White, *Inorg. Chim. Acta* **2003**, *352*, 143–150.

[7] a) B. J. Thomas, J. F. Mitchell, K. H. Theopold, J. A. Leafy, *J. Organomet. Chem.* **1988**, *348*, 333–342; b) P. de Frémont, N. Marion, S. P. Nolan, *J. Organomet. Chem.* **2009**, *694*, 551–560; c) N. Arnold, R. Bertermann, F. M. Bickelhaupt, H. Braunschweig, M. Drisch, M. Finze, F. Hupp, J. Poater, J. A. P. Sprenger, *Chem. Eur. J.* **2017**, *23*, 5948–5952.

[8] a) S. Schulz, T. Schoop, H. W. Roesky, L. Häming, A. Steiner, R. Herbst-Irmer, *Angew. Chem. Int. Ed. Engl.* **1995**, *34*, 919–920; b) S. Sinhababu, S. Kundu, A. N. Paesch, R. Herbst-Irmer, D. Stalke, I. Fernández, G. Frenking, A. C. Stückl, B. Schwederski, W. Kaim et al., *Chem. Eur. J.* **2018**, *24*, 1264–1268; c) H. Kameo, H. Yamamoto, K. Ikeda, T. Isasa, S. Sakaki, H. Matsuzaka, Y. García-Rodeja, K. Miqueu, D. Bourissou, *J. Am. Chem. Soc.* **2020**, *142*, 14039–14044.

[9] a) C. B. Caputo, L. J. Hounjet, R. Dobrovetsky, D. W. Stephan, *Science* **2013**, *341*, 1374–1377; b) F. P. Gabbaï, *Science* **2013**, *341*, 1348–1349; c) J. M. Bayne, D. W. Stephan, *Chem. Soc. Rev.* **2016**, *45*, 765–774; d) L. Greb, *Chem. Eur. J.* **2018**, *24*, 17881–17896.

[10] P. Erdmann, J. Leitner, J. Schwarz, L. Greb, *ChemPhysChem* **2020**, *21*, 987–994.

[11] a) P. Koelle, H. Noeth, *Chem. Rev.* **1985**, *85*, 399–418; b) W. E. Piers, S. C. Bourke, K. D. Conroy, *Angew. Chem. Int. Ed.* **2005**, *44*, 5016–5036; c) T. S. de Vries, A. Prokofjevs, E. Vedejs, *Chem. Rev.* **2012**, *112*, 4246–4282; d) P. Eisenberger, C. M. Crudden, *Dalton Trans.* **2017**, *46*, 4874–4887; e) Q. Zhao, R. D. Dewhurst, H. Braunschweig, X. Chen, *Angew. Chem. Int. Ed.* **2019**, *58*, 3268–3278; f) M. J. Ingleson in *Synthesis and Application of Organoboron Compounds* (Eds.: E. Fernández, A. Whiting), Springer International Publishing, Cham, **2015**; g) Y.-F. Lin, C.-W. Chiu, *Chem. Lett.* **2017**, *46*, 913–922.

[12] E. Vedejs, T. Nguyen, D. R. Powell, M. R. Schrimpf, *Chem. Commun.* **1996**, 2721.
[13] D. P. Curran, A. Solovyev, M. Makhlouf Brahmi, L. Fensterbank, M. Malacria, E. Lacôte, *Angew. Chem. Int. Ed.* **2011**, *50*, 10294–10317.
[14] a) B. Inés, M. Patil, J. Carreras, R. Goddard, W. Thiel, M. Alcarazo, *Angew. Chem. Int. Ed.* **2011**, *50*, 8400–8403; b) A. Prokofjevs, J. W. Kampf, A. Solovyev, D. P. Curran, E. Vedejs, *J. Am. Chem. Soc.* **2013**, *135*, 15686–15689.
[15] A. Röther, R. Kretschmer, *J. Organomet. Chem.* **2020**, *918*, 121289.
[16] a) Y. Yamaguchi, T. Kashiwabara, K. Ogata, Y. Miura, Y. Nakamura, K. Kobayashi, T. Ito, *Chem. Commun.* **2004**, 2160–2161; b) K. Ogata, Y. Yamaguchi, Y. Kurihara, K. Ueda, H. Nagao, T. Ito, *Inorg. Chim. Acta* **2012**, *390*, 199–209; c) S. Zlatogorsky, M. J. Ingleson, *Dalton Trans.* **2012**, *41*, 2685–2693.
[17] A J. Arduengo III, F. Davidson, R. Krafczyk, W. J. Marshall, R. Schmutzler, *Monatsh. Chem.* **2000**, *131*, 251–265.
[18] a) T. S. de Vries, E. Vedejs, *Organometallics* **2007**, *26*, 3079–3081; b) M. Brahmi, M. Malacria, D. Curran, L. Fensterbank, E. Lacôte, *Synlett* **2013**, *24*, 1260–1262.
[19] a) R. R. Holmes, R. N. Storey, *Inorg. Chem.* **1966**, *5*, 2146–2150; b) P. M. Treichel, R. A. Goodrich, S. B. Pierce, *J. Am. Chem. Soc.* **1967**, *89*, 2017–2022; c) R. Minkwitz, A. Liedtke, *Inorg. Chem.* **1989**, *28*, 4238–4242.
[20] J. W. Gilje, R. W. Braun, A. H. Cowley, *J. Chem. Soc. Chem. Commun.* **1974**, 15b.
[21] S. Villaume, A. Strich, S. A. Perera, R. J. Bartlett, *J. Phys. Chem. A* **2007**, *111*, 2220–2228.
[22] I. Krossing, H. Brands, R. Feuerhake, S. Koenig, *J. Fluorine Chem.* **2001**, *112*, 83–90.
[23] C. Y. Tang, A. L. Thompson, S. Aldridge, *J. Am. Chem. Soc.* **2010**, *132*, 10578–10591.
[24] a) T. E. Mallouk, G. L. Rosenthal, G. Mueller, R. Brusasco, N. Bartlett, *Inorg. Chem.* **1984**, *23*, 3167–3173; b) K. O. Christe, D. A. Dixon, D. McLemore, W. W. Wilson, J. A. Sheehy, J. A. Boatz, *J. Fluorine Chem.* **2000**, *101*, 151–153; c) I. Krossing, I. Raabe, *Chem. Eur. J.* **2004**, *10*, 5017–5030.
[25] J. C. Haartz, D. H. McDaniel, *J. Am. Chem. Soc.* **1973**, *95*, 8562–8565.
[26] H. C. Brown, N. Ravindran, *Inorg. Chem.* **1977**, *16*, 2938–2940.
[27] a) A. D. Becke, *Phys. Rev. A* **1988**, *38*, 3098–3100; b) T. H. Dunning, *J. Chem. Phys.* **1989**, *90*, 1007–1023; c) D. E. Woon, T. H. Dunning, *J. Chem. Phys.* **1993**, *98*, 1358–1371; d) R. A. Kendall, T. H. Dunning, R. J. Harrison, *J. Chem. Phys.* **1992**, *96*, 6796–6806; e) S. Grimme, S. Ehrlich, L. Goerigk, *J. Comput. Chem.* **2011**, *32*, 1456–1465.
[28] M.-A. Funke, H. Mayr, *Chem. Eur. J.* **1997**, *3*, 1214–1222.
[29] a) B. Blaser, K. H. Worms, *Angew. Chem.* **1961**, *73*, 76; b) J. Goubeau, R. Baumgärtner, H. Weiss, *Z. Anorg. Allg. Chem.* **1966**, *348*, 286–297.
[30] M. F. Klapdor, H. Beckers, W. Poll, D. Mootz, *Z. Naturforsch. B* **1997**, *52*, 1051–1054.
[31] H. Jiang, A. Bansal, R. Goyal, K.-W. Peng, S. J. Russell, T. R. DeGrado, *Bioorg. Med. Chem.* **2018**, *26*, 225–231.
[32] a) K. Chansaenpak, M. Wang, Z. Wu, R. Zaman, Z. Li, F. P. Gabbaï, *Chem. Commun.* **2015**, *51*, 12439–12442; b) D. M. Perrin, *Curr. Opin. Chem. Biol.* **2018**, *45*, 86–94.
[33] a) M. M. Brahmi, J. Monot, M. Desage-El Murr, D. P. Curran, L. Fensterbank, E. Lacôte, M. Malacria, *J. Org. Chem.* **2010**, *75*, 6983–6985; b) S. Sauerbrey, P. K. Majhi, J. Daniels, G. Schnakenburg, G. M. Brändle, K. Scherer, R. Streubel, *Inorg. Chem.* **2011**, *50*, 793–799.
[34] B. Hupp, J. Nitsch, T. Schmitt, R. Bertermann, K. Edkins, F. Hirsch, I. Fischer, M. Auth, A. Sperlich, A. Steffen, *Angew. Chem. Int. Ed.* **2018**, *57*, 13671–13675.
[35] a) Z. Otwinowski, W. Minor in *Methods in Enzymology:Macromolecular Crystallography Part A* (Ed.: C. W. Carter, Jr.), Academic Press, **1997**; b) COLLECT, Data Collection Software; Nonius B. V., Delft, The Netherlands, **1998**; c) SADABS 2.10, Bruker-AXS inc., **2002**, Madison, WI, U.S.A; d) C. H. Leung, C. D. Incarvito, R. H. Crabtree, *Organometallics* **2006**, *25*, 6099–6107; e) O. V. Dolomanov, L. J. Bourhis, R. J. Gildea, J. A. K. Howard, H. Puschmann, *J. Appl. Crystallogr.* **2009**, *42*, 339–341; f) G. M. Sheldrick, *Acta Crystallogr. Sect. C* **2015**, *71*, 3–8; g) G. M. Sheldrick, *Acta Crystallogr. Sect. A* **2015**, *71*, 3–8; h) A. L. Spek, *Acta Crystallogr. Sect. C* **2015**, *71*, 9–18; i) Gaussian 16, Revision C.01, M. J. Frisch, G. W. Trucks, H. B. Schlegel, G. E. Scuseria, M. A. Robb, J. R. Cheeseman, G. Scalmani, V. Barone, G. A. Petersson, H. Nakatsuji, X. Li, M. Caricato, A. V. Marenich, J. Bloino, B. G. Janesko, R. Gomperts, B. Mennucci, H. P. Hratchian, J. V. Ortiz, A. F. Izmaylov, J. L. Sonnenberg, D. Williams-Young, F. Ding, F. Lipparini, F. Egidi, J. Goings, B. Peng, A. Petrone, T. Henderson, D. Ranasinghe, V. G. Zakrzewski, J. Gao, N. Rega, G. Zheng, W. Liang, M. Hada, M. Ehara, K. Toyota, R. Fukuda, J. Hasegawa, M. Ishida, T. Nakajima, Y. Honda, O. Kitao, H. Nakai, T. Vreven, K. Throssell, J. A. Montgomery, Jr., J. E. Peralta, F. Ogliaro, M. J. Bearpark, J. J. Heyd, E. N. Brothers, K. N. Kudin, V. N. Staroverov, T. A. Keith, R. Kobayashi, J. Normand, K. Raghavachari, A. P. Rendell, J. C. Burant, S. S. Iyengar, J. Tomasi, M. Cossi, J. M. Millam, M. Klene, C. Adamo, R. Cammi, J. W. Ochterski, R. L. Martin, K. Morokuma, O. Farkas, J. B. Foresman, D. J. Fox, Gaussian, Inc., Wallingford CT, 2016; j) D. Kratzert, I. Krossing, *J. Appl. Crystallogr.* **2018**, *51*, 928–934.

Manuscript received: August 4, 2023
Accepted manuscript online: August 29, 2023
Version of record online: October 6, 2023